New Astronomy 82 (2021) 101453

Contents lists available at ScienceDirect

New Astronomy

journal homepage: www.elsevier.com/locate/newast

A new approximate coupling function: The case of Forbush decreases

L. Xaplanteris[a], M. Livada[a], H. Mavromichalaki[a,*], L. Dorman[b]

[a] Nuclear and particle Physics Department, Faculty of Physics, National and Kapodistrian University of Athens, Zografos, 15784 Athens, Greece
[b] Israel Cosmic Ray & Space Weather Centre and Emilio Segre Observatory, Tel Aviv University, Golan Research Institute and Israel Space Agency, Israel

ARTICLE INFO

Keywords:
Neutron monitors
Cosmic rays
Coupling functions
Forbush decreases

ABSTRACT

We attempt the derivation of a new coupling function between ground level and primary cosmic rays for the case of Forbush decreases. The calculations for the new function are based on basic Quantum Field Theory theoretical tools, something that has not been attempted till now in other widely used cosmic ray coupling functions. The use of Quantum Field Theory calculations in cosmic rays events in general, is expected to be a suitable frame of work since it describes well the high energy particle interactions which result in variations to the total number of the particles involved through annihilation or creation of particles. The newly computed function is tested to the case of two events of Forbush decreases, February 2011 and March 2012, using data from the high resolution neutron monitor database. Results for the primary particle intensity values obtained from this function are compared directly to the corresponding ones from the use of the Dorman's widely accepted coupling function. The two sets are discussed in detail in order to deduce the possible suitability of Quantum Field Theory tools to cosmic ray events.

1. Introduction

In this study the derivation of a new coupling function based on Quantum Field Theory (QFT) calculations is attempted for the case of Forbush decreases (Fds) of the cosmic ray intensity. These events were first discovered by Forbush (1937) and are short-duration cosmic ray events that were named after him. They become evident by a rapid decrease of the observed cosmic ray (CR) intensity by at least 2% (Forbush, 1954). A typical Fd lasts for a period of a few hours up to 2 days and the recovery time is of the order of a few days up to one week. Fds are generally believed to be caused by interplanetary coronal mass ejections from the Sun (Venkatesan and Badruddin, 1990; Kumar and Badruddin, 2014; Cane, 2000), which can also cause strong geomagnetic storms. The largest Fds are associated with coronal mass ejections (CMEs) that are accompanied by shock waves (e.g. Lockwood, 1971; Cane, 2000; Mavromichalaki et al., 2010; 2015; Papailiou et al., 2013). During their travel from the Sun to Earth, CMEs and their corresponding interplanetary CMEs interact with the galactic cosmic rays (GCRs) that fill the interplanetary space. The leading shock wave of the interplanetary CME (if any) and the following ejecta modulate the GCRs, which result in a reduced CR intensity (Cane, 2000; Badruddin, 2006).

The GCRs that manage to penetrate the Earth's atmosphere interact with its components and produce a plethora of secondary CRs that are measured by the ground based detectors. The coupling between the secondary particles with the primary ones is a very important task for the Space Weather research, done with the use of suitable coupling functions. Many different coupling functions have been proposed and used so far. Others based on theoretical calculations (e.g. Clem and Dorman, 2000), while others are derived by statistical and computational models e.g. Debrunner et al., 1982; Flückiger et al., 2008; Plainaki et al., 2009; Mishev and Velinov, 2011; Vashenyuk et al., 2011; Mishev et. al., 2013; Usoskin et al., 2015) . A few of the most widely used coupling functions are mentioned below:

- The function of Clem and Dorman (2000) that was computed numerically as the first detailed Monte-Carlo simulation using the FLUKA package
- The function of Caballero-Lopez and Moraal (2012) that was empirically constructed based on latitudinal surveys of a neutron monitor defined only for the rigidities below 15 GV
- The function of Mishev et al. (2013) that was computed using the PLANETOCOSMICS GEANT-4 simulation tool
- The function of Mangeard et al. (2016) that was computed using the FLUKA package
- The updated version of Mishev et al. (2013) function, extended to cover different atmospheric depths from sea level to 500 g/cm^2 (~5.7 km altitude) using parameterization techniques

* Corresponding author.
E-mail address: emavromi@phys.uoa.gr (H. Mavromichalaki).

https://doi.org/10.1016/j.newast.2020.101453
Received 1 May 2020; Received in revised form 10 July 2020; Accepted 12 July 2020
Available online 17 July 2020
1384-1076/

(Mishev et al., 2020)

In this work the derivation of a new coupling function based on some fundamental theoretical tools of QFT is attempted. QFT is a compatible framework for this case since it describes, by definition, high energy particle interactions in which the number and flavor of particles are not preserved (Peskin, 1995; Weinberg, 1995; Griffiths, 2008). More specifically the kind of the interactions that take place in Earth's atmosphere during the production of the secondary particles from the primary CRs, is considered. It is worth noting that an effort to derive a coupling function based on analytical QFT calculations, rather than calculations based on a classical approach or a Monte Carlo simulation model, is attempted.

The use of QFT is expected to yield interesting and more fitting results especially for the high energy region (>10 GeV). In the higher energies renormalization effects become evident in QFT, in which some physical quantities that were considered as constants are actually functions of the energy E (Bilal, 2011; Peskin, 1995; Griffiths, 2008). Taking into account these effects, the results may describe better the observed data of the secondary and primary particles.

After its computation, the new function is applied to two cases of Fds on February 2011 and March 2012. The goal of this work is the determination of the primary CRs in the heliosphere during these periods using the cosmic ray data of the secondary neutrons recorded by the neutron monitor (NM) stations. For the validation of the obtained results, they are compared directly with the corresponding ones using Dorman's coupling function (Dorman et al., 2000).

The structure of this work is as follows. Firstly, the data selection for the case of the Fds studied here, are given in Section 2. A brief description for each event is also given as well as the characteristics of neutron monitor stations whose data has been used. Then in Section 3 the newly proposed CR coupling function based on QFT calculations is described along with all the necessary assumptions taken into account for its computation. In Section 4 the application of the results to the case of the Fds, is presented. The results are compared to the corresponding ones using Dorman's widely accepted coupling function (Dorman et al., 2000; Villoresi et al., 2000). Lastly our results and comments on the use and application of QFT tools to CR problems are discussed. Additional improvements and expansions of the newly presented function are also proposed for the immediate future. Two appendices concerning the Neutron Monitors and the analysis of data are added.

2. Data selection

For the application of our results to the case of Forbush decreases of cosmic ray intensity, 6- and 12-hrs data of the cosmic ray intensity for five middle latitude neutron monitor stations during the examined Forbush decreases are considered (A. Belov et al., 2014; A. 2018). These data are obtained from the High resolution neutron monitor database (NMDB) (www.nmdb.eu) and the characteristics of the used stations (geographic coordinates, cut-off rigidity, and altitude) are given in Table 1. The selection of the stations was done according to the requirement of energy $E > 3$ GeV that corresponds to cut-off rigidity of $R > 3.8$ GV. In reality we are analyzed stations from 3.84 GV LMKS) to 8.53 GV (ATHN). We note that in the last column of Table 1 an altitude correction factor for each station is given.

The altitude of each station is a crucial parameter that affects the collected ground level data, so it has to be taken into account in our calculations. Stations with different altitudes would give different results for the primary spectrum. This problem was fixed in this work with the inclusion of an altitude correction factor calculated as follows: Assuming the upper limit of the atmosphere to be at 10 km and a station at altitude h (m), this means that the available distance for interactions above this station is 10.000-h (m). Considering as an example the Jungfraujoch station (JUNG, 3.570 m), the available path is roughly 64.3% of the total distance. So, in our final results the secondary flux $\delta N/N_0$ will have a factor of 0.643 in front of it. In order to eliminate this factor and deduce an altitude corrected primary flux δ_D/D_0, we include the inverse factor $1/0.643=1.555$. An analogous correction factor obtained with the same way was included only for the primary CR flux for each station. This factor offers a first approximation correction to our results.

The cases of Forbush decreases studie in this work are the ones of 18th February 2011 and of 8th March 2012. These events are selected to be in the ascending phase and in the maximum phase of the solar cycle 24, respectively. In every case the cosmic ray data were normalized to 2–3 days before the beginning of the event according to the relation

$$Ni = \frac{\delta N}{N_0} = \frac{N_{i0} - N_0}{N_0} \tag{1}$$

where N_0 is the average value of the measured secondary neutrons for these days prior to the beginning of the Fd. All of them are typical events and a short description of these Fds is given in the following:

a) **The Fd of February 2011:** The Fd of 18 February 2011 is the first significant one of solar cycle 24 and is recorded after an X-class flare (X2.2), that occurred on 15th February 2011 at 1:44 UT. The source of this Fd is a halo CME first recorded by SOHO/LASCO on 15/02/2011 at 2:24 UT with a velocity of 669 km/s. The amplitude of the Fd was 5.2% for 10 GV particles calculated by the Global Survey Method (Lingri et al., 2016; Belov et al., 2014; Papaioannou et al., 2018; Belov et al., 2018)

The time profile of the normalized cosmic ray intensity during the event of 17–22 February 2011 is given in the Fig. 1. Hourly corrected for pressure and efficiency values of the cosmic rays recorded at the ATHN, BKSN, JUNG, LMKS and ROME neutron monitor stations are normalized to the days 14, 15 and 16 of February 2011. Then we observe two different groups of stations concerning the amplitude of the Fd, the first one being from the stations ATHN (8.53 GV) and ROME (6.27 GV) and the second one from the stations JUNG (4.49 GV), LMKS (3.84 GV) and BKSN (5.70 GV).

a) **The Fd of March 2012:** The second Fd under study occurred on 8 March 2012 (Livada et al., 2018). This event is actually separated into two distinct decreases. The CME of 4 March 2012 at 11:00 UT was the first CME of a series of solar events that took place in the period from 4 to 12 of March 2012. The greater of them was

Table 1
Characteristics of the Neutron Monitor Stations used in this work.

Neutron Monitor Stations	Abbrev.	Cut-off Rigidity (GV)	Altitude (m)	Geographic coordinates	Altitude Cor. factor
Lomnicky Stit (Slovakia)	LMKS	3.84	2634	49.20° N 20.22° E	1.358
Jungfraujoch (Switzerland)	JUNG	4.49	3570	46.55° N 7.98° E	1.555
Baksan (Russia)	BKSN	5.70	1700	43.28° N 42.69° E	1.205
Rome (Italy)	ROME	6.27	0	41.86° N 12.47° E	1.000
Athens (Greece)	ATHN	8.53	260	37.97° N 23.78° E	
	1.027				

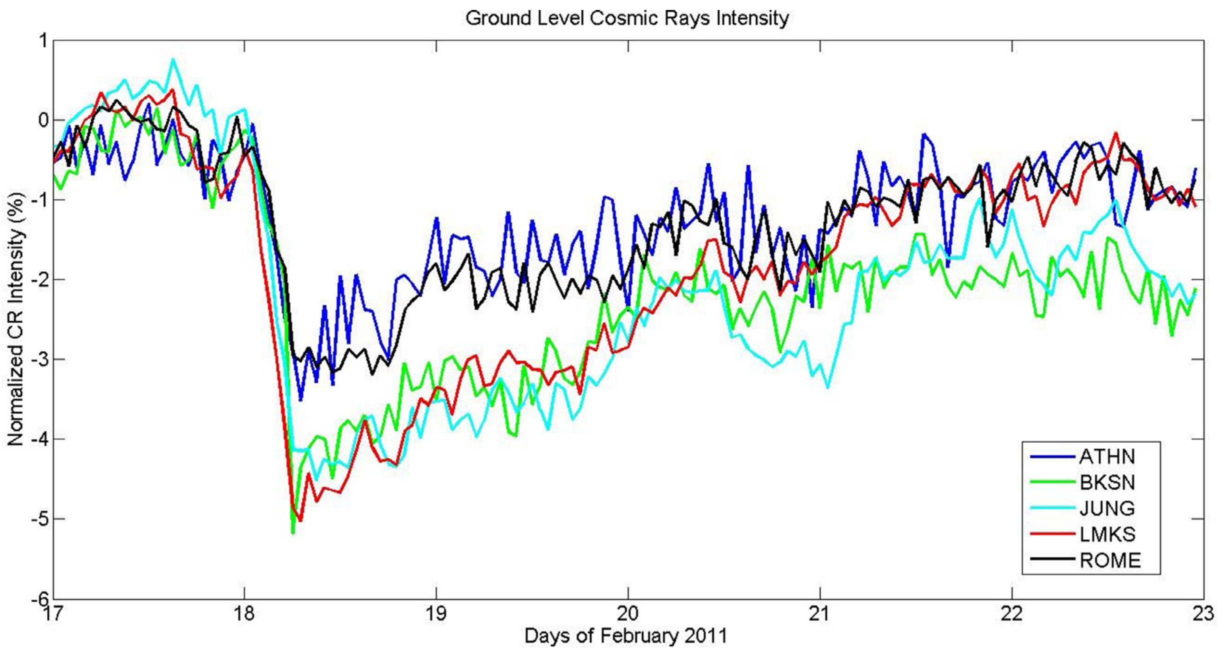

Fig. 1. Time profile of the normalized cosmic ray intensity for ATHN, BKSN, JUNG, LMKS and ROME NM stations for the time period 17- 22 February 2011.

associated with an X-ray flare (X5.4) occurred on 7 March 2012 at 00:02 UT. The first CME was recorded by SOHO/LASCO on 7 March 2012 at 00:24 UT reaching a speed of 2684 km/s. A little later at 01:30 UT, another CME was produced on the Sun with a velocity of 1825 km/s; this was associated with an X1.3 flare. As a result of the global disturbance, a severe geomagnetic storm took place when the shock arrived at Earth on 8 March 2012 at 11:05 UT.

The amplitude of the Fd on this day was reached to the value of 12%. The hourly corrected for pressure and efficiency values of the cosmic ray intensity recorded at the neutron monitor stations are normalized to the days 5 and 6 of March 2012 before the beginning of the Fd on 8 of March. The normalized values of CRs versus time are presented in Fig. 2. It is noted that again the cosmic ray intensity of the stations of ATHN and ROME was recorded during these Fds with a smaller amplitude than the one recorded by the other three stations of JUNG, LMKS and BKSN.

3. The new coupling function

The initial step of the calculations is the choice of a suitable Lagrangian density, $\mathcal{L}$, which can describe the interactions between the primary and the secondary particles. For simplicity we assume that the primary particles are solely protons and they produce only secondary neutrons. With that assumption the $\mathcal{L}$ of this study is:

$$L = \frac{1}{2}(\partial_\mu \Phi_1)^2 + \frac{1}{2}(\partial_\mu \Phi_2)^2 + \frac{1}{2}m_1^{\,2}\Phi_1^2 + \frac{1}{2}m_2^2\Phi_2^2 - \frac{\lambda}{2!2!}\Phi_1^2\Phi_2^2 \tag{2}$$

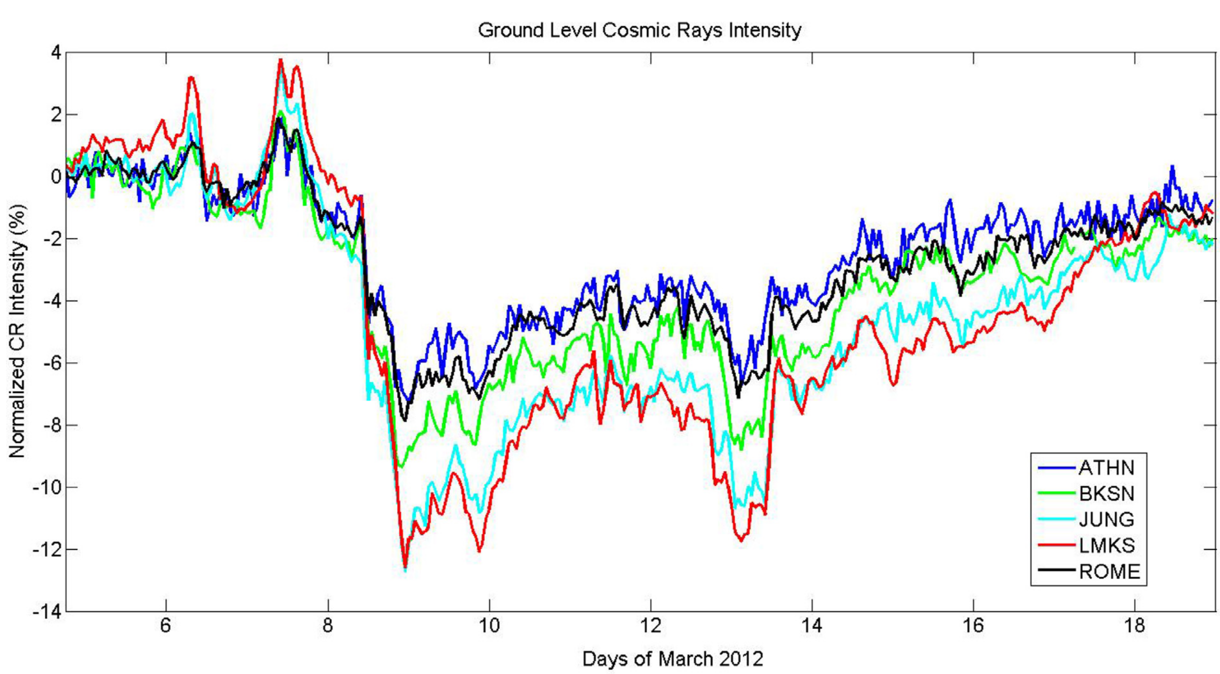

Fig. 2. Time profile of the normalized cosmic ray intensity for ATHN, BKSN, JUNG, LMKS and ROME stations for the time period 5- 18 March 2012.

where Φ_1, Φ_2 are the scalar fields representing the primary proton and secondary neutron, m_1,m_2 their respective masses and λ, the interaction constant of our theory.

We note that this particular form of $\mathcal{L}$ is actually a slight variation of the commonly found -φ^4 theory (with interaction term $V(\varphi) \sim \varphi^4$) (Peskin, 1995; Srednicki, 2007; Bilal, 2011). The reason for choosing this fairly basic form of the Lagrangian is once again because we wanted to test the applicability of Quantum Field Theory's most fundamental principles to realistic CR problems. More advanced concepts (e.g. Dirac fields, more realistic and complicated interaction terms, inclusion of more fields corresponding to different particles etc.) are the subject of future analysis.

Next we introduce the counter-terms of our theory: Z_1, Z_2, Z_{m1}, Z_{m2}, Z_λ which will absorb the divergences of the calculations (Peskin, 1995; Weinberg, 1995).

For the determination of the coupling function only the Z_λ counter-term is needed.

$$Z_\lambda = Z_1 Z_2 \frac{\hat{\lambda}_0}{\hat{\lambda}} \tag{3}$$

After the introduction of the counter-terms, we compute the 4-point Green's function, $G^{(4)} = \langle\Phi_1\Phi_2\Phi_1\Phi_2\rangle$, (Peskin, 1995; Bilal, 2011) which describes the interaction between the primary proton and the secondary neutron in the form of : $p \to p + n + \bar{n}$. The contributing Feynman diagrams for the 4-point function in 1-loop approximation are: which give us the counter-term :

$$Z_\lambda = 1 + \frac{3\hat{\lambda}}{16\pi^2}\left(\frac{1}{\varepsilon} - \gamma + 2\ln(4\pi) + \ldots\right) \tag{4}$$

where $\varepsilon \to 0$, is the divergent part of our computations and $\gamma = 0.5772$, the Euler-Mascheroni constant ('t Hooft and Veltman, 1972; 't Hooft, 1973). We also find $Z_1 = Z_2 = 1$.

Then from the renormalization group equations (Srednicki, 2007; Bilal, 2011) of our theory we derive the analytical expression for the coupling constant of our $\mathcal{L}$ as a function of the energy of the primary proton.

$$\hat{\lambda} = \frac{\hat{\lambda}_0}{1 - \frac{3\hat{\lambda}_0}{8\pi^2}\ln\left(\frac{E}{E_{cut}}\right)} \tag{5}$$

The quantity $\hat{\lambda}_0$ will be determined below.

The total 4-point Green's function is found to be:

$$G^{(4)} = -i(2\pi)^4\hat{\lambda} \tag{6}$$

The next step is the expansion of our results for the case of multiple interactions, so that a primary proton can produce a number of secondary neutrons.

The primary protons reach the upper limit of Earth's atmosphere moving towards the surface. In their way, they interact with atmospheric particles (such as O_2, N_2 etc.) thus producing many secondary particles. In this paper we focus only on the production of secondary neutrons, assuming only the particle interaction, $p^+ \to p^+ + n + \bar{n}$, meaning a primary proton produces a new proton (with less energy) and a pair of neutron and anti-neutron. We focus only on this specific interaction for simplicity of computations. This process continues to repeat itself as long as the proton has sufficient energy to produce the three particles. So, by assuming this simple model we have the production of multiple secondary neutrons from one primary proton.

The secondary neutrons are produced in different layers in the atmosphere (first secondary neutron upper layer, second neutron lower layer, etc.) and they eventually reach the ground detectors (neutron monitors). They are produced in different atmospheric heights.

Moreover we note that inside the neutron monitor we also have the production of neutrons from the Pb rings that surround the detectors. But this production of neutrons inside the detector is not the main focus of this work. We emphasize primarily in the production of neutrons in the atmosphere in order to determine if our assumed model yields realistic results. A more detailed description of a neutron monitor is given in Appendix A.

More specifically we assume that after each interaction the primary proton loses a constant percentage of its energy equal to 40% (Dorman, 1974), thus it is able to repeat the process a finite number of times. With this assumption the energy of the proton is calculated by a geometrical series of the form:

$$E_n = 0.6^n E_0$$

where E_0 is the initial energy of the proton, n is the number of interactions, E_n the energy of the proton after n interactions.

We also take into account that the energy of the primary proton has to be sufficient for the production of at least one secondary neutron, so we assume an energy cut-off of:

$$E_{cut} = 3\,\text{GeV}$$

From these assumptions we determine the factor $\frac{\ln(\frac{E_{cut}}{E})}{\ln(0.6)}$ which is added to the coupling function (6).

Lastly, in order to deduce the scattering amplitude from the coupling function (6), we use the Lehmann, Symanzik, Zimmermann (LSZ) formula (Peskin, 1995; Srednicki, 2007; Bilal, 2011):

$$S_{fi} = \prod_{i=1}^{m}\frac{1}{\sqrt{2E_i}}\frac{1}{(2\pi)^{3/2}}G^{(4)}\prod_{j=1}^{n}\frac{1}{\sqrt{2E_j}}\frac{1}{(2\pi)^{3/2}} \tag{7}$$

where i runs over all primary particles (in our case just 1 proton), j runs over all secondary produced particles (in our case 3) with E_i, E_j their corresponding energies.

Expression (7) squared is the corresponding coupling function between primary CRs (protons) and secondary neutrons derived from the QFT calculations, as a function of the energy E of the primary proton.

$$W(E, \hat{\lambda}_0) = 3.8*10^{-4}*\frac{1}{E^3}*\left(\frac{\ln\left(\frac{E_{cut}}{E}\right)}{\ln(0.6)}\right)^2*\left(\frac{\hat{\lambda}_0}{1 - \frac{3\hat{\lambda}_0}{8\pi^2}\ln\left(\frac{E}{E_{cut}}\right)}\right)^2 \tag{8}$$

The first check is given in Fig. 3, where the newly computed function is compared to the one in Dorman et al. (2000):

$$W(R) = akR^{-(k+1)}\exp(-aR^{-k}) \tag{9}$$

with $\begin{matrix} a = 10.275 \\ k = 0.9615 \end{matrix}$ for NM

We note that the constant $\hat{\lambda}_0$ would be normally determined by the normalization condition of the coupling function when it is integrated over all energy spectrum:

$$\int_0^\infty |S_{fi}|^2 dE = 1$$

but since this function is valid only for energies $E > 3$ GeV, we simply choose $\hat{\lambda}_0$ to be equal to 1, so it is of the same order with Dorman's coupling function. Thus, Eq. (8) becomes:

$$W(E) = 3.8*10^{-4}*\frac{1}{E^3}*\left(\frac{\ln\left(\frac{E_{cut}}{E}\right)}{\ln(0.6)}\right)^2*\left(\frac{1}{1 - \frac{3}{8\pi^2}\ln\left(\frac{E}{E_{cut}}\right)}\right)^2 \tag{10}$$

We note that the two functions seem to be in accordance in the energy region: 3 GeV $< E <$ 1000 GeV with the new function being slightly above Dorman's function. This slight difference is thought to be caused by the renormalization effects that become evident in QFT (Weinberg 1995; Peskin, 1995). This higher value of the newly computed function is also believed to yield better results for the calculated CR intensities, thus correcting in a fully theoretical way some discrepancies observed in some events between the collected ground level

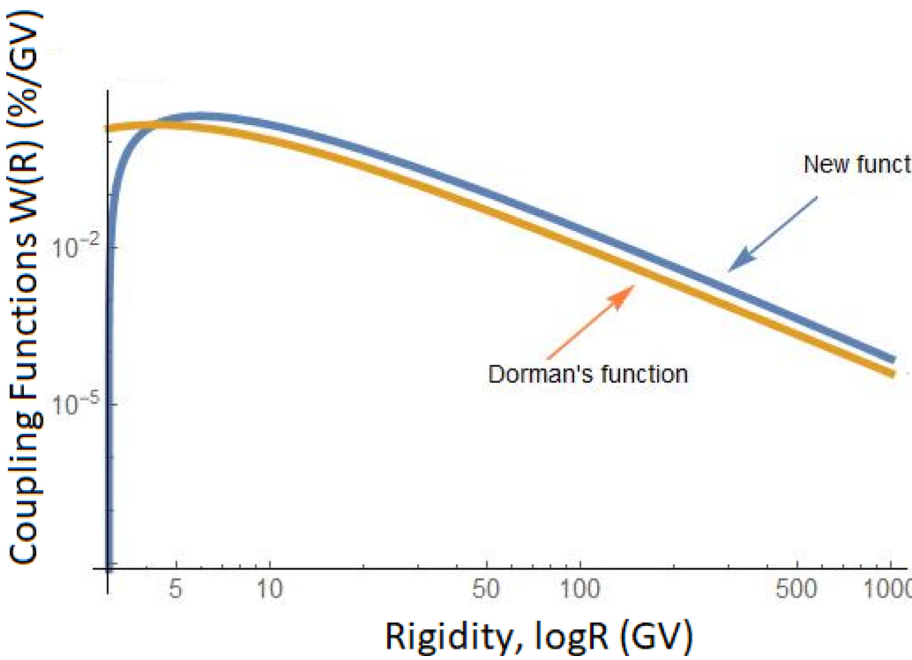

Fig. 3. Direct comparison between the Dorman's coupling function and the newly derived one based on fundamental QFT calculation for energies above 3 GeV, is presented.

data with the expected ones using other coupling functions (Villoresi et al., 2000). One final comment regarding the newly computed function is the energy region in which the function is valid. Function (10) is valid from energy $E > E_{cut} = 3$ GeV up to the energy value that vanishes the denominator of Eq. (10). The critical energy value for which the denominator becomes zero, is called the Landau pole (Peskin, 1995; Weinberg, 1995) of this function and it is calculated to

$$1 - \frac{3}{8\pi^2}\ln\left(\frac{E_L}{E_{cut}}\right) = 0 \rightarrow E_L = E_{cut}\exp\left(\frac{8\pi^2}{3}\right) = 7.8{*}10^{10}GeV$$

It is resulted that the function (10) is valid in the energy region: $3\text{ GeV} < E < 7.8 \times 10^{10}$ GeV.

4. Application to Forbush decreases

The procedure that we followed is to apply the coupling function to the cosmic ray data of each station and thus to derive the amplitude of the primary cosmic ray spectrum for that point of time.

The newly computed function of Eq. (10) is applied to the cases of the two Fds discussed above. The obtained results are compared with the corresponding ones using Dorman's function of Eq. (9).

The analysis is based on Dorman's equation which correlates the secondary particles with the primary ones using the coupling coefficient

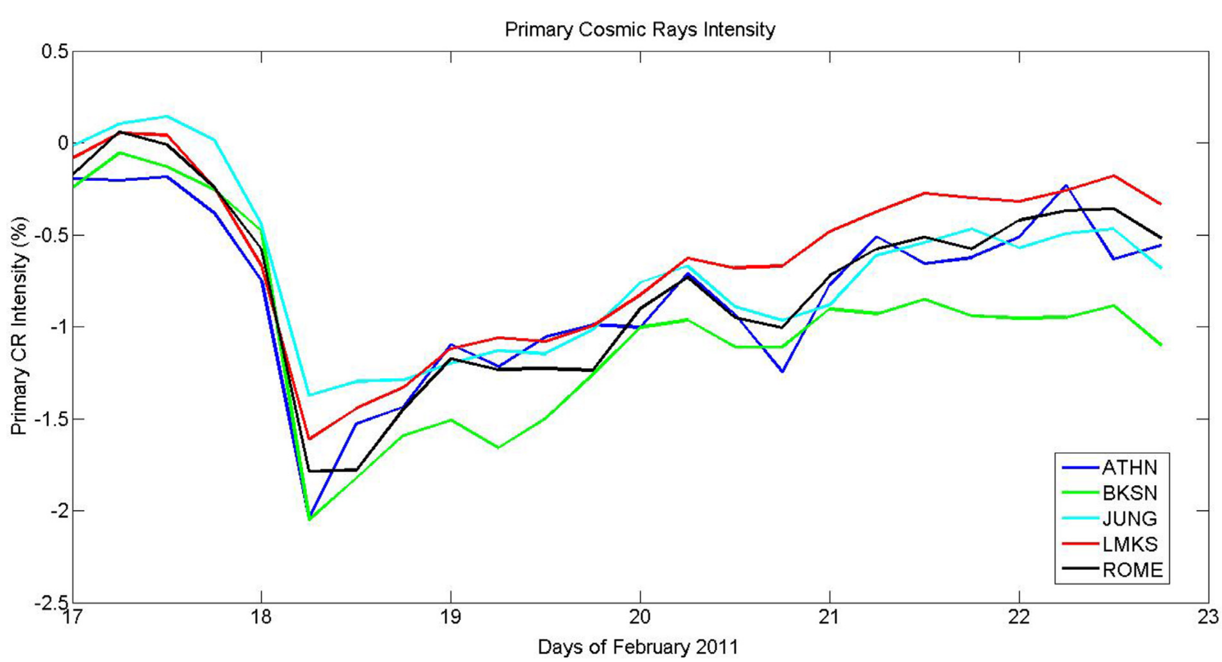

Fig. 4. a: Time profile of the cosmic ray intensity in the heliosphere using the new coupling function of Eq. (11). b: Time profile of the cosmic ray intensity in the heliosphere using Dorman's coupling function of Eq. (9).

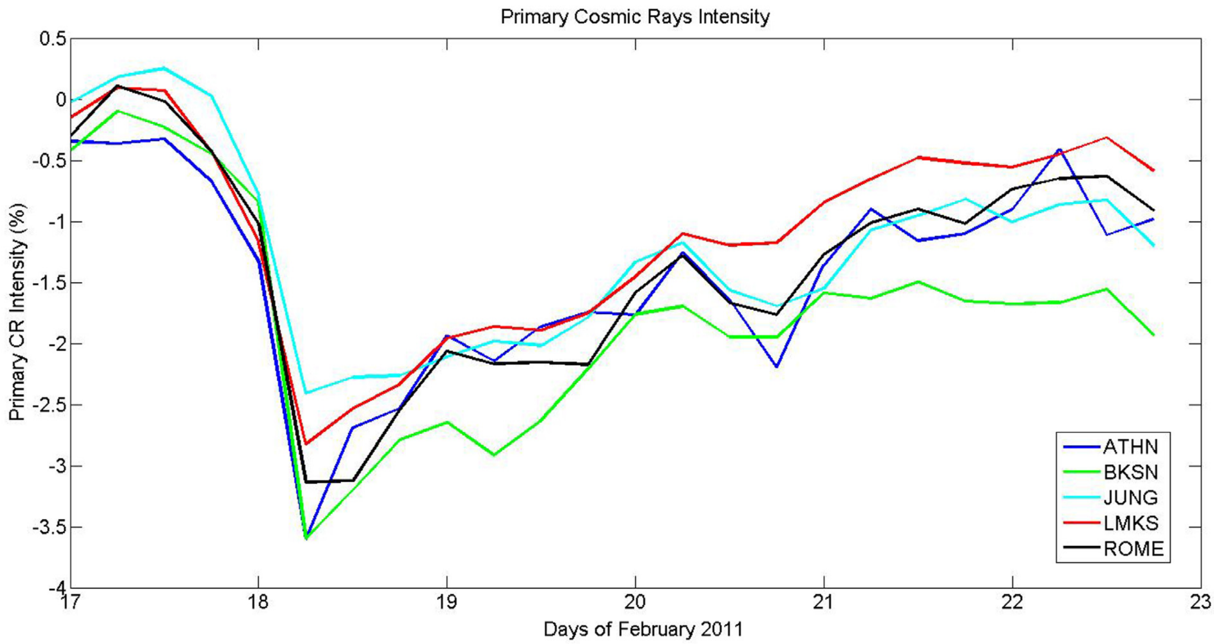

Fig. 4. (*continued*)

method. The coupling coefficient method was introduced by Dorman (1974) and it is one of the most widely used methods of determining the primary CRs spectrum outside Earth's atmosphere. The theoretical approach of this method is expected to be consistent with the theoretical approach followed thus far in this study.

The full analytical procedure followed in this work is presented in Appendix B. Here we give the final results obtained from the new coupling function with rigidity R as a free parameter (instead of energy E):

$$W(R) = 3.8*10^{-4}*\frac{1}{\sqrt{R^2+1}^{3}}*\left(\frac{\ln\left(\frac{E_{cut}}{\sqrt{R^2+1}}\right)}{\ln(0.6)}\right)^2*\left(\frac{1}{1-\frac{3}{8\pi^2}\ln\left(\frac{\sqrt{R^2+1}}{E_{cut}}\right)}\right)^2 \tag{11}$$

And the final relation between the primary and secondary particle intensities:

$$J(t) = \int_0^t \frac{\delta D_t}{D_0}(t)dt = \frac{\gamma-1}{kR_c^{1-\gamma}}\frac{1}{\int_{R_c}^{\infty} W(R)dR}\frac{\delta N}{N_0}(t) \tag{12}$$

For the application of our results to the case of Forbush decreases of

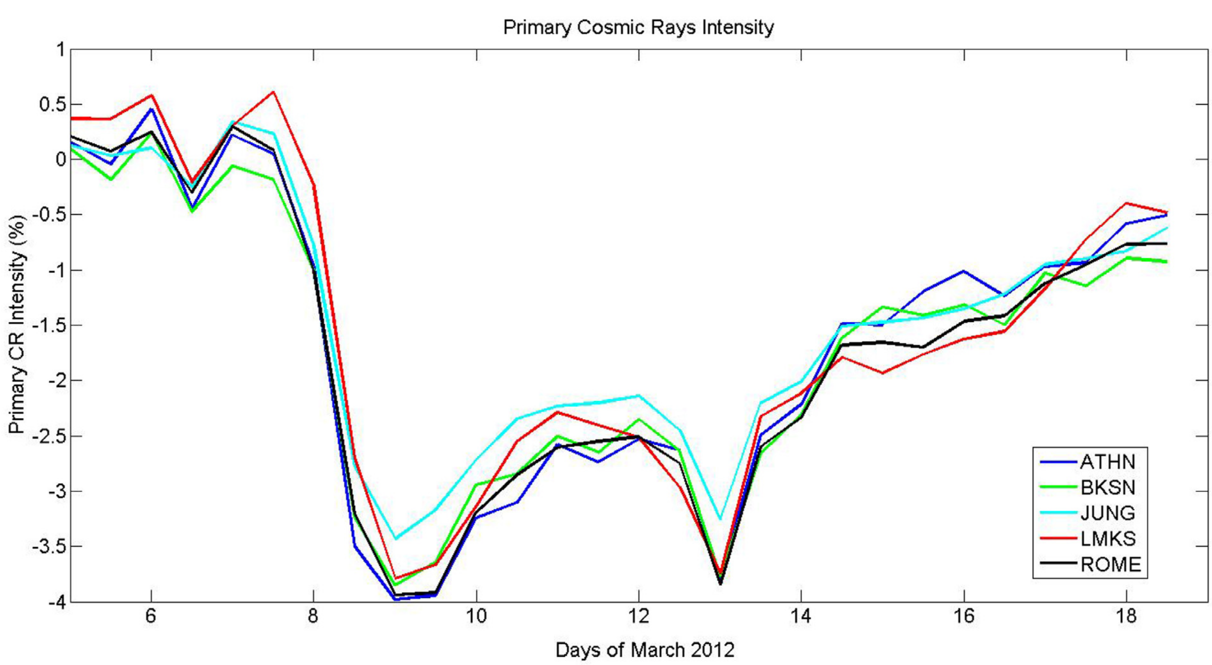

Fig. 5. a: Time profile of the cosmic ray intensity in the heliosphere using the new coupling function of Eq. (11). b: Time profile of the cosmic ray intensity in the heliosphere using Dorman's coupling function of Eq. (9).

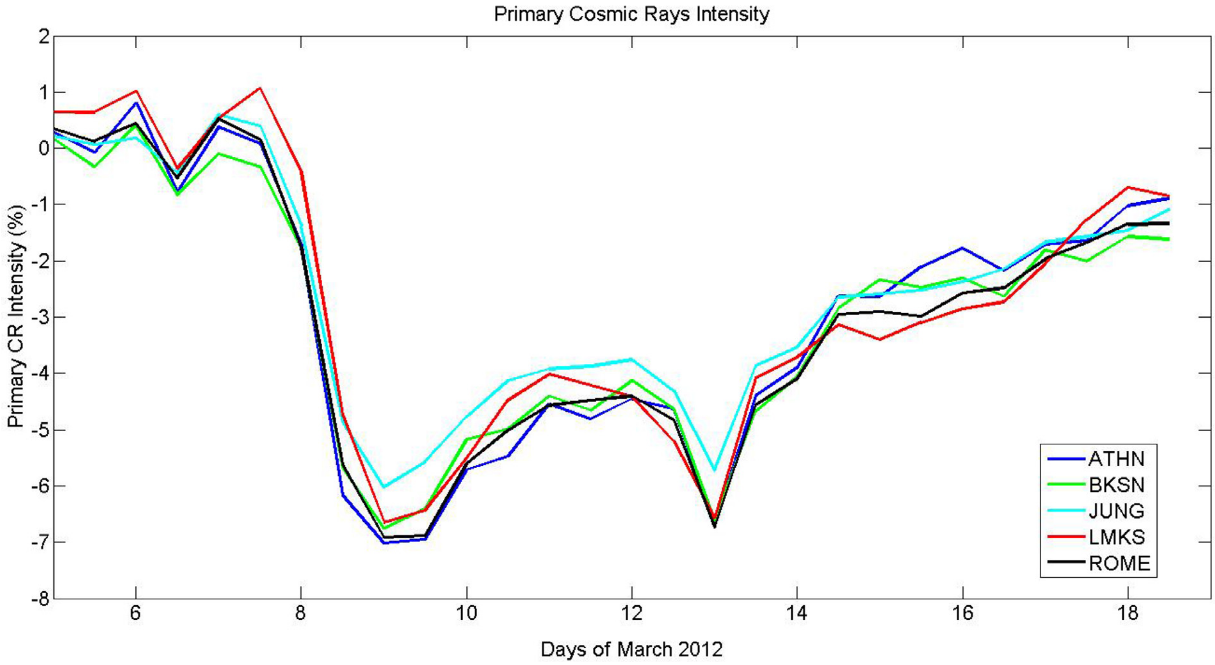

Fig. 5. (*continued*)

cosmic ray intensity we consider 6- and 12-hourly data values of the cosmic ray intensity obtained from the High resolution neutron monitor database -NMDB (www.nmdb.eu) for the five middle latitude neutron monitor stations (Table 1).

a) Forbush decrease of February 2011: By substituting in Eq. (12) the new function of Eq. (11) and the Dorman's function of Eq. (9), we find out the following results for the primary particles summarized in Table 2.

Firstly, we note that the results of the primary CR intensities have the same structure with the ground level CR intensity presented in Fig. 1, using both coupling functions. That is an initial result of great importance for the validity of the analytical method used in this work, as well as for the newly computed function. We then note that the values for the primary CR amplitudes for each station are significantly closer with one another (compared to the corresponding values for the ground level measurements) using both functions, as can be seen in Table 2. In the last row of Table 2 we present the absolute difference in the amplitude of the primary CR, meaning the difference between the highest and lowest calculated values among all stations using both functions. This coincidence of the primary CR intensities from every station is to be expected because outside Earth's atmosphere the effects that modulate the values of the secondary CRs (e.g. air concentration, meteorological effects) do not take place. So the calculated primary intensity is expected to be similar for every station. We also note that the coincidence of the primary CRs using the new function (11) is better (the results from all station differ only 0.68% with one another) than the one found using Dorman's function (9) (the results differ 1.19%). This is another important result since one of the initial goals of this work was the improvement of existing widely known coupling functions, such as Dorman's, with the use of QFT computations. Lastly we note that the results for the primary CR amplitude using the new function have in general lower values than the ones using Dorman's function. This is caused due to the fact that the newly computed function takes higher values for the energy region under study ($E >$ 3 GeV) than Dorman's function. That causes the integral in the denominator of Eq. (12) to be greater for the case of the new function, so the value of the fraction, which is essentially the function of the primary CR amplitude with time, is decreased. b) **Forbush decrease of March 2012:** The results for the primary particle flux using the two functions under study as well as the calculated results in Table 3:

Once again we note that the primary CR intensities using both functions follow the behavior of the ground level CR intensity as it is shown in Fig. 2. Moreover the values for the primary CR intensities for each station are again significantly closer with one another compared to the corresponding values for the ground level measurements using both functions, as we can see in Table 3. In this particular event the coincidence of the primary particles' intensities is even better than before,

Table 2
The amplitude of the Forbush decrease recorded at every station and the corresponding values for the primary data using the new function as well as Dorman's function.

NM Stations	Fd Amplitude (%)	Primary CR Amp. (%) New Function	Primary CR Amp. (%) Dorman et al. (2000)
ATHN	3.03	2.04	3.60
BKSN	4.36	2.05	3.60
JUNG	4.25	1.37	2.41
LMKS	4.72	1.61	2.83
ROME	3.01	1.79	3.14
Absolute Amplitude Difference	1.71	0.68	1.19

Table 3
The amplitude of the Forbush decrease as recorded from each station and the corresponding values for the primary data using the new function as well as Dorman's function.

NM Stations	Fd Amplitude (%)	Primary CR Amp. (%) New Function	Primary CR Amp. (%) Dorman et al. (2000)
ATHN	5.89	3.98	7.02
BKSN	8.18	3.85	6.76
JUNG	10.63	3.43	6.02
ROME	6.64	3.94	6.92
LMKS	11.08	3.79	6.65
Absolute Amplitude Difference	5.19	0.55	1.00

as can be seen in both the figures and the last row of Table 3. Once again the calculated absolute difference of the amplitude of the primary intensities is better (0.55%) using the newly computed function of Eq. (11) compared to the one using Dorman's function of Eq. (9), (1.00%).

5. Conclusions and future improvements

In this paper a new coupling function for CR was computed analytically for the first time using fundamental QFT calculations. After its computation it was tested for the case of two typical Fd events. More specifically the primary particle flux was deduced from the normalized CR data from five middle latitude neutron monitor stations. The primary particle flux was compared with the corresponding results using Dorman's (Dorman et al., 2000) widely used coupling function. The results are in good accordance in both cases which is very optimistic for further application of even more advanced QFT concepts and results in CR events.

More specifically, the primary CR intensities followed the form of the ground level normalized CRs in both events which was the first positive result. Moreover the calculated amplitudes of the primary CRs for each station were found similar to one another. This result is important, as the coincidence of the primary CR intensity for all neutron monitor stations was expected, due to the lack of atmospheric modulation outside the Earth's atmosphere causing the splitting of the values of the ground level CR intensity. The results using the newly computed function were satisfactory and even better that the corresponding ones using Dorman's function. This last result is the most important and promising for further use and application of our newly computed function. We note that the newly computed function follows the same analytical approach as that of Dorman's (Dorman and Zukerman, 2003; Dorman, 2004) but considering high energy (renormalization) effects, something that seems to improve the existing results, at least for the case of Fds for now.

The next step of this study will be the improvement of this newly obtained function considering the altitude (h) of each neutron monitor station as a new parameter of the coupling function. With this introduction of the altitude, the results of the primary flux are expected to be even better and closer among all stations. In addition the use of altitude correction factors, such as the ones used here (Table 1), will be not necessary.

Moreover an attempt to include more contributing interactions that result in the production of secondary particles will be attempted. This specific improvement is thought to be the most challenging one due to increased complications in calculations. But it will certainly correspond to a more realistic model for the production of the secondary CR particles.

Lastly, the expansion/extrapolation of the coupling function for the energy region below to 3 GeV will be attempted, in order to be applicable for polar and low-latitude neutron monitor stations as well. This expansion will be made by either analytical extrapolation of the new function of Eq. (11) in the low energy region below to 3 GeV or by a change in the initial assumptions of the simplistic theoretical model used in this article.

Concluding, we can say that an initial step for a new coupling fuction has been made and a coupling function in its early form determined solely on fundamental QFT analytical calculations yielded encouraging and promising results in the first application on realistic CR events.

CRediT authorship contribution statement

L. Xaplanteris: Conceptualization, Formal analysis, Writing - original draft. **M. Livada:** Methodology, Data curation. **H. Mavromichalaki:** Supervision, Validation, Writing - review & editing. **L. Dorman:** Writing - review & editing.

Declaration of Competing Interest

The authors declare that they have no conflict of interest.

Acknowledgments

Many thanks are due to our collaborators of the Neutron Monitor stations for kindly providing the cosmic ray data used in this work in the frame of the High resolution real time Neutron Monitor database NMDB, funded under the European Union's FP7 Program (contract no. 213007). Athens Neutron Monitor Station (A.Ne.Mo.S. http://cosray.phys.uoa.gr/) is supported by the Special research account of the National and Kapodistrian University of Athens.

Supplementary materials

Supplementary material associated with this article can be found, in the online version, at doi:10.1016/j.newast.2020.101453.

Appendix A

A neutron monitor is a ground-based instrument designed to measure secondary neutrons produced by the interaction of cosmic rays and solar energetic particles with the atmospheric molecules. Each neutron monitor is characterized by its altitude above sea level and its vertical cut-off rigidity.

The neutron, as a particle with no electric charge, makes interactions only with nuclei and can therefore penetrate large layers of material without interactions because of the small range of the strong nuclear force (Malandraki and Crosby, 2018). After a hadronic interaction of an energetic neutron with a nucleus, the excited target nucleus emits so-called evaporation neutrons. In a material containing nuclei with low atomic mass, the neutrons are effectively slowed down (moderated) in elastic collisions. These facts led Simpson (1958) to the neutron monitor detector concept: production of fast neutrons in a target with high atomic weight, braking of the fast neutrons in a hydrogenous material, and finally detection of the thermic neutrons indirectly by ionizing particles that are produced in a neutron induced nuclear reaction.

The different components of a neutron monitor detector are:

Reflector: The task of the reflector is to reflect and to moderate the evaporation neutrons that are produced in the lead producer. In addition, this neutron monitor component has the function to reflect and to absorb the low energy neutrons that are produced in the neutron monitor.

Producer: The core of the neutron monitor consists of a lead producer, a target with high atomic mass (A), to produce secondary neutrons. These neutrons amplify the cosmic ray signal and cannot easily escape the reflector. The lead producer is interspersed with a moderator and the BF_3 proportional counter tubes.

Moderator: Each counter tube is surrounded by a polyethylene tube acting as a moderator for the evaporation neutrons that are generated in the lead producer.

Proportional Counter: The proportional counter tubes are filled with BF_3 as counter gas enriched with ^{10}B When the slow neutrons encounter a ^{10}B nucleus in the proportional counter, the following favored reaction may take place:

$${}^{10}_{5}B + n \rightarrow {}^{7}_{3}Li + {}^{4}_{2}He$$

The produced α-particle and the Li-nucleus are accelerated by the applied high voltage within the counter tube, ionize the counter gas and the produced electrons cause an electric signal (Simpson, 2000; Carmichael, 1968; Mavromichalaki et al., 2001).

A global distribution of neutron monitors transforms the Earth in a spectrometer that allows to estimate the energy spectrum of the cosmic ray flux arriving at Earth. The Neutron Monitor Database (NMDB) is a joint effort to create a database of high resolution data from neutron monitor stations located over the world (Mavromichalaki et al., 2011; Blanco et al., 2019).

Appendix B

We present in detail the analytical procedure followed in order to obtain the final relation between the secondary and primary cosmic rays intensities.

The initial point of the coupling coefficient method which is the starting point of our calculations, is that any component I of the secondary CRs (in our study only neutron) that is detected in atmospheric altitude h is described by the relation (Dorman et al., 2000):

$$N_i(R(t), h(t), t) = \int_{R_c(t)}^{\infty} D(R, t) m_i(R, h(t), g(t), T(h, t), E(h, t)) dR \tag{B.1}$$

where R is the cut-off rigidity of each station

D is the primary spectrum of CRs outside Earth's atmosphere
m_i is the integral multiplicity of the i component of CRs as a function of the rigidity R, gravitational acceleration g, temperature T and atmospheric electrical field E.

The integral multiplicity m_i is defined as the total number of secondary particles (in our case neutrons) that are produced by only 1 primary particle (in our case proton) with a defined initial energy.

Using the definition of Eq. (B.1) any variation of the detected CR intensity can be attributed to each of the three parameters inside the integral:

$$\delta N_i(R(t), h(t), t) = \int_{R_c(t)}^{\infty} D(R, t) \delta m_i(R, h(t), g(t), T(h, t), E(h, t) dR$$
$$- \delta R_c(t) D(R, t) m_i(R, h(t), g(t), T(h, t), E(h, t)) + \int_{R_c(t)}^{\infty} \delta D(R, t) m_i(R, h(t), g(t), T(h, t), E(h, t)) dR \tag{B.2}$$

In this particular work we will focus only on the variations caused by the last term of the right hand side, meaning variations caused by the δ_D term which are known as variations of the primary CRs spectrum.

By introducing the quantity

$$W(R_c, h) = \frac{D(R) m_i(R, h, g, T(h), E(h)}{N_i} \tag{B.3}$$

We obtain the relative variation of the CRs:

$$\frac{\delta N_i}{N_{i0}}(t) = \int_{R_c}^{\infty} \frac{\delta D}{D_0}(R, t) W(R) dR \tag{B.4}$$

Where $\frac{\delta N_i}{N_{i0}}$: is the normalized cosmic ray flux
$\frac{\delta D}{D_0} = \frac{D - D_0}{D_0}$: is the normalized primary CR flux
$W(R)$: coupling function as defined by Dorman
R: rigidity

We note that the integration in Eq. (B.4) is over the term of cut-off rigidity and so we can perform a change of the variable E in Eq. (10) with the variable of the rigidity R.

Using the definition of the rigidity $R = \frac{pc}{Ze}$, where pc is the relativistic momentum of the primary protons and Ze is its charge.

From the relation $E = \sqrt{p^2c^2 + m^2c^4}$, we find that $E = \sqrt{R^2Ze^2 + m^2c^4}$

For protons $Ze = 1$ and $m \approx 1 GeV$, also taking $c = 1$, we have:

$$E = \sqrt{R^2 + 1}$$

Thus, the function (10) becomes:

$$W(R) = 3.8 * 10^{-4} * \frac{1}{\sqrt{R^2 + 1}^3} * \left(\frac{\ln\left(\frac{E_{cut}}{\sqrt{R^2+1}}\right)}{\ln(0.6)} \right)^2 * \left(\frac{1}{1 - \frac{3}{8\pi^2} \ln\left(\frac{\sqrt{R^2+1}}{E_{cut}}\right)} \right)^2 \tag{11}$$

In Eq. (B.1) the normalized secondary data are obtained from the NMDB network as a function of time: $\frac{\delta N}{N_0} = \frac{\delta N}{N_0}(t)$

So, the primary data $\frac{\delta D}{D_0}$ can be determined. We assume that the primary particles have the form: $\frac{\delta D}{D_0}(R, t) = \int_0^t \frac{\delta D_t}{D_0}(t) dt \int_0^R \frac{\delta D_R}{D_0}(R) dR$, that means that the term $\frac{\delta D}{D_0}$ can be separated into two parts, one time dependent and one rigidity (energy) dependent. The rigidity dependent part of $\frac{\delta D}{D_0}$ can be determined analytically from the primary particle flux relation:

$$J(R) = kR^{-\gamma} \quad \text{(B.5)}$$

With $\gamma \approx 2.5$, the energy spectrum exponent and $k \approx 500$

Using Eq. (B.5), we find $\int_{R_c}^{\infty} \frac{\delta D_R}{D_0}(R)dR = \int_{R_c}^{\infty} kR^{-\gamma}dR = k\frac{R_c^{1-\gamma}}{\gamma-1}$

So, the equation (B.4) becomes:

$$\frac{\delta N}{N_0}(t) = k\frac{R_c^{1-\gamma}}{\gamma-1}\int_{R_c}^{\infty} W(R)dR\int_0^t \frac{\delta D_t}{D_0}(t)dt \Rightarrow$$

$$J(t) = \int_0^t \frac{\delta D_t}{D_0}(t)dt = \frac{\gamma-1}{kR_c^{1-\gamma}}\frac{1}{\int_{R_c}^{\infty} W(R)dR}\frac{\delta N}{N_0}(t) \quad (12)$$

the primary particle flux as a function of time t, meaning the number of primary protons per energy, per solid angle as a function of t.

References

Badruddin, 2006. Transient perturbations and their effects in the heliosphere, the geomagnetosphere, and the Earth's atmosphere: space weather perspective. J. Astrophys. Astron. 27, 209. https://doi.org/10.1007/BF02702523.

Belov, A., Eroschenko, E., Yanke, V., Oleneva, V., Abunin, A., Abunina, M., Papaioannou, A., Mavromichalaki, H., 2018. The global survey method applied to ground-level cosmic ray measurements. Sol. Phys. 293, 68. https://doi.org/10.1007/s11207-018-1277-6.

Belov, A., Abunin, A., Abunina, M., Eroshenko, E., Oleneva, V., Yanke, V., Papaioannou, A., Mavromichalaki, H., Gopalswamy, N., Yashiro, S., 2014. Coronal mass ejections and non-recurrent forbush decreases. Sol. Phys. 289, 3949. https://doi.org/10.1007/s11207-014-0534-6.

Bilal, A., 2011, Advanced quantum field theory: renormalization, non-abelian gauge theories and anomalies, Lect. Notes Brus..

Blanco, J.J., Medina, J., Garcia Poblacion, O., Gomez Herrero, R., Garcia Tejedor, J.I., et al., 2019. A new neutron monitor at the juan carlos i spanish antarctic station (Livingston Island-Antarctic Peninsula). In: 36th International Cosmic Ray Conference -ICRC2019-. U.S.A.

Caballero-Lopez, R., Moraal, H., 2012. Cosmic-ray yield and response functions in the atmosphere. J. Geophys.Res 117, A 12103. https://doi.org/10.1029/2012JA017794.

Cane, H.V., 2000. Coronal mass ejections and Forbush decreases. Space Sci. Rev. 93, 55. https://doi.org/10.1023/A:1026532125747.

Carmichael, H., 1968, in C. M. Minnis (ed.), Cosmic Rays (Instruments), Annals of the IQSY1, 178–197.

Clem, J.M., Dorman, L.I., 2000. Neutron monitor response functions. Space Sci. Rev. 93, 335. https://doi.org/10.1023/A:1026508915269.

Debrunner, H., Fluckiger, E.O., Lockwood, J., 1982. Specific Yield Function S(P) For a Neutron Monitor At Sea Level. Proc. 8th Europe Cosmic Ray Symp., Rome, preprint.

Dorman, L.I., 1974. Cosmic Rays Variations and Space Explorations. North-Holland Publishing Company.

Dorman, L.I., 2004, Cosmic Rays in the Earth's Atmosphere and Underground, 216, Kluwer Academic Publishers, Dordrecht, 10.1007/978-1-4020-2113-8.

Dorman, L.I., Zukerman, T., 2003. Initial concept for forecasting the flux and energy spectrum of energetic particles using ground-level cosmic ray observations. Adv. Space Res. 31, 925. https://doi.org/10.1016/S0273-1177(02)00799-8.

Dorman, L.I., Villoresi, G., Iucci, N., et al., 2000. , Cosmic ray survey to Antarctica and coupling functions for neutron component near solar minimum (1996-1997) 3. Geomagnetic effects and coupling functions. J. Geophys. Res 105 (A9,), 21047. https://doi.org/10.1029/2000JA900051.

Flückiger, E.O., Moser, M.R., Pirard, B., Bütikofer, R., Desorgher, L., 2008, A parameterized neutron monitor yield function for space weather applications, Proc. 30 th ICRC 2007, 1289.

Forbush, S.E., 1937. On the effects in cosmic-ray intensity observed during the recent magnetic storm. Phys. Rev 51, 1108. https://doi.org/10.1103/PhysRev.51.1108.3.

Forbush, S.E., 1954. Worldwide cosmic ray variations, 1937–1952. J. Geophys. Res. 59, 525. https://doi.org/10.1029/JZ059i004p00525.

Griffiths, D., 2008. Introduction to Elementary particles, Weinheim. Wiley-VCH, Germany, 9783527406012.

't Hooft, .G.., 1973. Dimensional regularization and the renormalization group. Nucl. Phys B 61, 455. https://doi.org/10.1016/0550-3213(73)90376-3.

't Hooft, G., Veltman, M.J.G., 1972. Regularization and Renormalization of Gauge Fields. Nucl. Phys., B 44, 189. https://doi.org/10.1016/0550-3213(72)90279-9.

Kumar, A., Badruddin, 2014. Cosmic-Ray Modulation due to High-Speed Solar-Wind Streams of Different Sources, Speed, and Duration. Solar Phys 289. https://doi.org/10.1007/s11207-014-0565-z.

Lingri, D., Mavromichalaki, H., Belov, A., Eroshenko, E., Yanke, V., Abunin, A., Abunina, M., 2016. Solar Activity Parameters and Associated Forbush Decreases During the Minimum Between Cycles 23 and 24 and the Ascending Phase of Cycle 24. Solar Phys 291, 1025. https://doi.org/10.1007/s11207-016-0863-8.

Livada, M., Mavromichalaki, H., Plainaki, C., 2018. Galactic cosmic ray spectral index: the case of Forbush decreases of March 2012,. Astrophys. Space Sci 363, 8. https://doi.org/10.1007/s10509-017-3230-9.

Lockwood, J.A., 1971. Forbush decreases in the cosmic radiation. Space Sci .Rev 12, 658. https://doi.org/10.1007/BF00173346.

Malandraki, O.E., Crosby, N.B., 2018, Solar particle radiation storms forecasting and analysis, Springer International Publishing, 444. 10.1007/978-3-319-60051-2.

Mangeard, P.S., Ruffolo, D., Saiz, A., Nuntiyakul, W., Bieber, J.W., Clem, J., Humble, J.G., 2016. Dependence of the neutron monitor count rate and time delay distribution on the rigidity spectrum of primary cosmic rays. J. Geophys. Res., Space Phys 121, 11620. https://doi.org/10.1002/2016JA023515.

Mavromichalaki, H., Gerontidou, M., Paschalis, P., Papaioannou, A., Paouris, E., Souvatzoglou, G., 2015. Research applications of the Athens neutron monitor system. J. Phys. Conf. Ser. 632, 012071.

Mavromichalaki, H., Souvatzoglou, G., Sarlanis, C., Mariatos, G., Papaioannou, A., Belov, A., Eroshenko, E., Yanke, V., for the NMDB team, 2010. Implementation of the ground level enhancement alert software at NMDB database. New Astronomy 15, 744–748. https://doi.org/10.1016/j.newast.2010.05.009.

Mavromichalaki, H., Sarlanis, C., Souvatzoglou, G., Tatsis, S., Belov, A., Eroshenko, E., Yanke, V. and Pchelkii, A., 2001, "Athens neutron monitor and its aspects in the cosmic-ray variations", Proc. 27th ICRC 2001 (Hamburg)10, 4099–4102.

Mavromichalaki, H., Papaioannou, A., Plainaki, C., Sarlanis, C., Souvatzoglou, G., Gerontidou, M., Papailiou, M., Eroshenko, E., Belov, A., Yanke, V., Flückiger, E.O., Bütikofer, R., et al., 2011. Applications and usage Of the real – time neutron monitor database. Adv. Space Res 47, 2210–2222.

Mishev, A.L., Koldobskiy, S.A., Kovaltsov, G.A., Gil, A., Usoskin, I.G., 2020. Updated Neutron-Monitor Yield Function: bridging Between In Situ and Ground-Based Cosmic Ray Measurements. J. Geophys. Res. Space Phys 125. https://doi.org/10.1029/2019JA027433. e2019JA02743.

Mishev, A.L., Usoskin, I.G., Kovaltsov, G.A., 2013. Neutron monitor yield function: new improved computations. J. Geophys. Res. Space Phys. 118, 2783. https://doi.org/10.1002/jgra.50325.

Mishev, A.L., Velinov, P.I.Y., 2011. Normalized ionization yield function for various nuclei obtained with full Monte Carlo simulations. Adv. Space Res 48, 19. https://doi.org/10.1016/j.asr.2011.02.008.

Papailiou, M., Mavromichalaki, H., Abunina, M., Belov, A., Eroshenko, E., Yanke, V., Kryakunova, O., 2013. Forbush decreases associated with western solar sources and geomagnetic storms: a study on precursors. Solar Phys 283, 557. https://doi.org/10.1007/s11207-013-0231-x.

Papaioannou, A., Anastasiadis, A., Sandberg, I., Jiggens, P., 2018. Nowcasting of solar energetic particle events using near real-time coronal mass ejection characteristics in the framework of the FORSPEF tool. Space Weather Space Clim. 8, A 37. https://doi.org/10.1051/swsc/2018024.

Peskin, M.E., Schroeder, D.V., 1995. An Introduction to Quantum Field Theory. Perseus Books.

Plainaki, C., Mavromichalaki, H., Belov, A., Eroshenko, E., Yanke, V., 2009. Modeling the solar cosmic ray event of 13 December 2006 using ground level neutron monitor data. Adv. Space Res 43 (4), 474. https://doi.org/10.1016/j.asr.2008.07.011.

Simpson, J.A., 1958. 'Cosmic Radiation Neutron Intensity Monitor', Annals of the Int. Geophysical Year IV, Part VII, Pergamon. Press, London 351.

Simpson, J.A., 2000. The Cosmic Ray Nucleonic Component: the Invention and Scientific Uses of the Neutron Monitor. Space Sci. Rev 93, 11–32.

Srednicki, M., 2007. Quantum Field Theory. Cambridge University Presshttps://doi.org/10.1017/CBO9780511813917.

Usoskin, I.G., Kovaltsov, G.A., Adriani, O., Barbarino, G.C., Basilevskaya, G.A., et al., 2015. Force-field parameterization of the galactic cosmic ray spectrum: validation for Forbush decreases, Adv. Space Res 55, 2940. https://doi.org/10.1016/j.asr.2015.03.009.

Vashenyuk, E.V., Balabin, Y.V., Germanenko, A.V., et al., 2011. , Predicting dangerous radiation fluxes of solar cosmic rays on the basis of data from neutron monitors, Bull. Russ. Acad. Sci. Phys. 75, 770. https://doi.org/10.3103/S1062873811060426.

Venkatesan, D., Badruddin, 1990. Cosmic-ray intensity variations in the 3-dimensional heliosphere. Space Sci. Rev. 52, 121. https://doi.org/10.1007/BF00704241.

Villoresi, G., Dorman, L.I., Iucci, N., Ptitsyna, N.G., 2000. Cosmic ray survey to Antarctica and coupling functions for neutron component near solar minimum (1996-1997) 1., Methodology and data quality assurance. J. Geophys. Res 105, 21. https://doi.org/10.1029/2000JA900048. 025-21, 034.

Weinberg, S., 1995. The Quantum Theory of Fields Vol.I. Cambridge University Press.